SAND2008-1753C

High Energy Density Laser Interactions with Planetary and Astrophysical Materials: Methodology and Data

John L. Remo

Harvard University Dept. of Astronomy and Dept. of Planetary Sciences and Harvard Smithsonian Center for Astrophysics, 60 Garden St. Cambridge MA 02138, USA, mail stop18, jremo@cfa.harvard.edu and Sandia National Laboratories, PO box 5800, mail stop 1193, Albuqerque, NM 87185; jlremo@sandia.gov
and
Richard G. Adams
Sandia National Laboratories, PO box 5800, mail stop 1193
Albuqerque, NM 87185; rgadams@sandia.gov

ABSTRACT

Sandia National Laboratories NLS (1064 nm) and Z-Beamlet (527 nm) pulsed lasers @ ~ 100 GW/cm^2 and 10 TW/cm^2 were used to attain pressures at 20 – 525 GPa on a variety of metallic and mineral targets. A simple, inexpensive and innovative electro-optical real-time methodology monitored rear surface mechanical deformation and associated particle and shock wave velocities that differ considerably between metals and non-metals. A reference calibration metal (Aluminum) and a reference non-metal (graphite) were used to demonstrate the validity of this methodology. Normative equations of state and momentum coupling coefficients were obtained for dunite, carbonaceous meteorites, graphite, iron and nickel. These experimental results on inhomogeneous materials can be applied to a variety of high energy density interactions involving stellar and planetary material formation, dynamic interactions, geophysical models, space propulsion systems, orbital debris, materials processing, near-Earth space (Lunar and asteroid) resource recovery, and near-Earth object mitigation models.

Keyword List: Momentum coupling, equations of state, shock wave measurements

Objective

The objective of this paper is to outline and establish validity for application of a simple, inexpensive, and innovative electro-optical real time method to thick (> mm) targets to determine normative equations of states (EOS) and momentum coupling coefficients (C_M) under high energy density radiation (HEDR) driven pressure and temperature for metal, dielectrics, and inhomogeneous and anisotropic materials having applications in astrophysical, geophysical, and planetary evolution modeling and material alteration studies such as shock driven melt and element migration [1,2]. Since planetary materials are inhomogeneous, EOS and C_M deviate within normative ranges. Direct application of these results include near-Earth (Lunar, comet, and asteroid) space resource recovery [3], (nuclear and ion) propulsion systems simulation, astrodynamic modeling, and near-Earth object (NEO) hazard mitigation [4] processes involving HEDR.

Experimental method

Experiments were carried out using electro-optic real-time experimental techniques to monitor responses of mesoscale (~ 3 mm in radius and ~ 1-2 mm thick) target materials driven by high energy density laser radiation from ~ 0.20 to 13.4 TW/cm^2 to determine EOS and C_M at high pressures (20-525 GPa). A description of the overall experimental set-up is shown in figure 1. Scattered laser light from a pulsed laser beam impacting the front surface is detected and initiates a time sequence that records an optical signal from a continuous wave probe laser beam reflecting from the rear surface and received by a detector. Initiation of the signal reduction from the rear surface as recorded by

the detector through a narrow acceptance angle fiber optic probe indicates shock wave (SW) arrival at the diamond turned rear target surface. On target rear surfaces where no additional reflectors are needed (such as aluminum), the target rear surface faces a vacuum and the push out velocity is twice the rear surface particle velocity. For all other nonreflecting targets the probe laser beam is directly reflected from an Al/BK7 mirror in contact with the target rear surface, and the push out velocity ~ the particle velocity. The diode probe laser beam is inserted and collected along a narrow acceptance angle (less than 0.1 degree) through commercially available fiber optics with a lens on the beam acceptance aperture and a photodetector on the detection end. Push out time for the particle velocity is determined by measuring the time from the shock wave arrival to the time taken for the signal to reach its minimal value, indicating complete probe laser beam displacement from the detector by the rear surface movement (~ 30 μm). In metals often up to three such push out/pull back (ringing) cycles can be observed. This generally does not occur for dielectrics and certainly not for powders.

Because the very high intensity levels (10's TW/cm^2) generate high pressures (~ 100's GPa), great care must be taken to properly ground and shield electronic instruments from spurious radiation signals, including electromagnetic pulses resulting from front surface plasma generation that can obscure measurements and even burn out instruments [5]. Since the targets are thick, ~ 1 mm , electromagnetic signals from the HEDR laser beam do not affect rear surface reflectivity. An advantage of this optical displacement method over the point visar technique (more appropriate for thin ~ 10 μm targets where front surface intensity affects rear surface reflectivity) is that sampling is not point or even line dependent, as is point or line visar that can generate skewed results by sampling only one or two of many different phases [6]. The rear surface displacement method measures rear surface gross deformation including (mineral) phases and inclusions.

Computation of the momentum coupling coefficient

The momentum coupling coefficient, C_M, on the target front surface is given by

$$C_{M\,pl} = P_{pl} / I \qquad (1)$$

where P_{pl} is the laser induced plasma pressure on the target front surface by radiation intensity I (PW/cm^2), wavelength λ(μm), atomic mass A, and atomic number Z; where, assuming full ionization [8],

$$P_{pl} = 4.8\ (I/\lambda)^{2/3}\ (A/(Z+1))^{1/3} \qquad (2)$$

C_M at the rear surface is obtained from

$$C_{M\,H} = P_H / I \qquad (3)$$

where P_H is the Hugoniot pressure given by

$$P_H = \rho_o\, u_p\, u_s\ . \qquad (4)$$

Equation (4) is the EOS relationship of the Hugoniot pressure, P_H, as a function of particle velocity, u_p, SW velocity, u_s, and uncompressed target density ρ_o. The compressed target density, ρ, is determined from ρ_o using

$$\rho = \rho_o / (1 - u_p/u_s) \qquad (5)$$

Experimental results

Experiments on the solid metal targets, (Al in particular) and the non-metal solid targets served as a calibration for this methodology to electro-optically measure in real time shock wave and rear surface particle velocities. In figures 2 a,b the lower intensity NLS laser @ 570 GW/cm^2, 70 ns pulse induces a resonance within the target periodically ringing the rear surface while the higher intensity, 6.38 TW/cm^2, 235 ns pulse Z-Beamlet (ZBL) laser beam overdrives the Al target with no ringing.

EOS relationships of Hugoniot pressure, P_H, are plotted with respect to particle velocity, u_p, SW velocity, u_s, and compressed target density ρ for Al in figures 3a,b,c. C_M as a function of intensity is plotted in figure 3d.

The much higher energy density ZBL laser has a reduced coupling as can be observed in table 1 which clearly shows the reduced momentum coupling at the higher intensities. Experimental results for the rear surface particle

velocity, EOS relationships and C_M, for Al, Fe, Ni, dunite, graphite, and carbonaceous chondrite (meteorites) are summarized in table 1 for metallic and non-metallic targets. Theoretically, $C_M \sim (I/\lambda)^{-2/3}$.

Strain rates

Pressures generated on Al target rear surfaces at ~ 10s GPa generate strain rates,

$$d\varepsilon/dt = (d\delta/\tau_+) / \delta \qquad (6)$$

where $d\varepsilon/dt = (30\mu/\tau_+)/\delta \approx 3.5 - 7 \times 10^6$ /s in the non-spall regime, depending on intensity and target thickness. High power laser experiments on aluminum[9] with strain rates from 10^3 /s to 10^6 /s in pre-spall regimes and $\sim 10^7$ /s in spall regimes used 50 μm thick targets, ~ 1/20 the NLS target thickness and ~ 1/37 the ZBL thickness experiments. Since the strain rate is inversely proportional to target thickness, 50μm targets would be expected to yield strain rates beyond 10^7 /s. Future experiments with 50 -100 μm targets will measure spall velocities and associated strain.

Normative properties

Table 2 compares EOS parameters obtained by the laser irradiation using simple optical deflection techniques with a gas gun. For a given P_H these values indicate the method in this research for the measurements of the SW velocity and the particle velocity exhibits considerable scatter possibly due to the non-uniformity in the laser beam. This level of scatter is not useful for precisely determining EOS but is very helpful in estimating normative values that can be used for planetary and astrophysical modeling. This simple instrumentation method is well suited for measuring EOS parameters for inhomogeneous targets with inherent scatter due to different phases. The theoretical relationship between shock wave and particle speeds is given by

$$u_s = v + s\, u_p + \ldots \qquad (7)$$

where v is the speed of sound and s = 1.34 for Al. When $P_H = 0$, $u_p = 0$ and $u_s = v$. Laser pressure generated in the plasma zone expands (and dissipates) as it propagates through the target while a gas gun flat plat impactor generates a planar pressure pulse. As shown in table 2, u_s and u_p vary more because of this effect[7,10].

.

Interpretations

When interpreting results of laser driven EOS parameters and momentum coupling, one must understand that the irregularities in the spatial and temporal pulse shape will affect the plasma pressure that drives the SW. Even small perturbations or aberrations in laser beam quality (uniformity) can induce substantial changes in beam intensity homogeneity and subsequent material responses. Irregularities in the target further amplify these irregularities. The linear displacement of the rear surface from which the rear surface probe laser beam monitors displacement will be affected. This is why it is realistic to accept normative response of the EOS parameters for such interactions.

There is an inverse relationship between laser intensity and momentum coupling coefficient. For example, in figure 2 the relatively lower NLS intensity (< 1 TW/cm^2) on the Al target allows a more distinct EOS target response of target higher order rear surface reverberations (ringing). However, the more intense ZBL intensity (> 5 TW/cm^2) overdrives the target and provides the shock wave and particle velocities only to the first order. These results provide a level of consistency and accuracy that supports the methodology and suggests these simulation results can be applied to a broad range of astrophysical, geophysical, planetary science, and space technology problems

Since the three different materials groups analyzed exhibit characteristically different behaviors when subjected to the same laser irradiations, these factors must be taken into account when modeling in astrophysical and planetary processes. Even within a single material group there are significant variances associated with chemical and molecular structure changes. Shock driven melt and element migration from miscibility altered siderophile and lithophile compounds were observed. Such effects have important implications for planet formation and exoplanet structure where pressures and temperatures drive zone melting and species migration are important indicators [1,2].

The overall response of the EOS variables of the inhomogeneous materials was normative, clustering about a mean value. This is not surprising since these experiments are on mesoscale samples where inhomogeneities, imperfections, voids, and grain boundaries effect observations and contribute to a lack of exact reproducibility of

EOS response for materials that are otherwise similar from the perspective of categorization. Results for the laser irradiations are similar to high intensity hohlraum shots [6], suggesting that HEDR lasers may be valid surrogates for blackbody solar, planetary collision, near-Earth object mitigation, and stellar radiation.

Conclusions

These experiments validate use of an optical deflection method to extract normative EOS and C_M responses for various inhomogeneous materials. EOS values obtained are broadly consistent with those obtained from hypervelocity flyer plate interactions for the same P_H values [7,10], suggesting that although HEDR laser interactions and associated high pressure surface plasmas that generate compression (shock) waves are qualitatively different from mechanical impact pressures that generate compression waves, the closeness of the EOS is acceptable. Because these targets are (non-microscopic) objects that have grain and phase boundaries, voids or porosity, responses within specific materials categories vary, but tend to cluster around normative values with limited variance. Normative scatter from inhomogeneous targets also characterizes point and line visar yielding dispersed data due to distinct phase sampling. Sensitivity and accuracy from optical displacement probe detectors can be improved with symmetric laser probe/ detectors positioned on opposite sides of the back surface, i.e. each probe reflects from only one (opposite) side of the displaced surface. This will detect asymmetries in the measurements.

We thank Ian Smith and the ZBL Operations crew at Sandia National Laboratories for excellent assistance in conducting these experiments and John Porter for his support in this work. This work was partially supported by NNSA research contract DE-FG52-66NA26215 with Harvard University.

References

1. M. I. Petaev, Jacobsen, S. B., Remo, J. L., and R.G. Adams, "Experimental study of high energy processing of protoplanetary materials," **AGU/DPS**, 2006; M. I. Petaev, S. B. Jacobsen, J. L. Remo, and R. G. Adams, "Experimental study of high energy processing of protoplanetary materials," **Lunar Planet. Sci. Conf** . **XXXVIII**, 1822, 2007; M. I. Petaev , S. B. Jacobsen, J. L. Remo, R. G. Adams, and D. D. Sasselov, "Experimental study of high energy processing of protoplanetary materials: implications for the post-giant impact earth," **Lunar Planet. Sci. Conf**, **XXXIX**, 2008**.**

2. J. L. Remo, R.G. Adams, M. I. Petaev, and S. B. Jacobsen, "Laser simulation of high P-T planetary processes," **AGU/DPS**, Dec 2006; J. L. Remo, R.G. Adams, M. I. Petaev, and S. B. Jacobsen, "Laser simulation of high P-T planetary processes: physics of laser induced shocks in solid and powdered targets, **Lunar Planet. Sci. Conf**. **XXXVIII**, 1822, 2007; J. L. Remo, R.G. Adams, M. I. Petaev, and S. B. Jacobsen, "Experimental simulation of high P-T planetary processes, **Lunar Planet. Sci. Conf**. **XXXIX**, April 2008.

3. L. Gertsch, J. L. Remo, and R. Gertsch, "Asteroid/Comet Classification for Mining Purposes," **Earth and Space 2006**, paper in press 2006.

4. Remo, J.L., editor., "**Near Earth Objects: The United Nations International Conference,** Annals of the N.Y. Acad.Sc., **822,** (1997).

5. Remo, J. L., R.G. Adams, M. C. Jones, "Atmospheric electromagnetic pulse propagation effects from thick targets in terawatt laser target chamber," **Applied Optics, 46,** 6166- 6175, 2007

6. J. L. Remo and M. D. Furnish, "High intensity X-ray coupling to meteorite targets," 1410-1413, Intl. J. Impact Engnrg, **Proc. HVIS** 2001,2002; J. L. Remo and M. D. Furnish, "High intensity X-ray coupling to meteorite targets," 1410-1413, Intl. J. Impact Engnrg, **Proc. HVIS** 2001, 2002; J. L. Remo and M. D. Furnish, "Analysis of Z-pinch shock wave experiments in meteorite and planetary materials," in press Intl. J. Impact Engnrg, **Proc. HVIS,** 2007, 2008; J. L.. Remo and M. D. Furnish, "Analysis of Z-pinch shock wave experiments in meteorite and planetary materials," in press 2008.

7. Meyer, M. A., Dynamic Behavior of Materials, Wiley, NY, 1994.

8. Atzeni, S. and Meyer-ter-Vehn, J., The Physics of Inertial Fusion, Clarendon Press, Oxford, 2004.

9. Eliezer, S., I. Gilath, and T. Bar-Noy, J. Appl. Phys., 67, 715, 1990.

10. Marsh, S. P. ed, LASL Shock Hugoniot Data, U. Cal. Press, Berkeley, 1980.

Figures

Figure 1. Experimental configuration for electro-optic real time shock wave and particle velocity measurements using direct reflection form the rear target surface

Figure 2a. Electro-optic real-time measurements for the shock wave arrival, 280 ns, and push-out time, 70 ns, for the NLS 1064 nm laser irradiation of an Al target at 570 GW/cm^2 .

Figure 2b. Electro-optic real-time measurements for the shock wave arrival, 235 ns, and push-out time, 34 ns for the ZBL 527 nm laser irradiation of an Al target at 6.38 TW/cm^2.

Figure 3a. Equations of state for laser irradiations of Al: Shock wave speed u_s as a function of Hugoniot Pressure P_H. Also shown is the linear least-square best fit.

Figure 3b. Particle speed u_p as a function of P_H and its linear best fit.

Figure 3c. Compressed density ρ as a function of P_H and its linear best fit.

Figure 3d . Momentum coupling coefficient C_M as a function of intensity and its best fit.

Target	I	δ	λ	P_{pl}	$C_{M\,pl}$	P_H	u_s	u_p	ρ	$C_{M\,H}$
Al	0.33	0.490	1064	27	0.82	17.7	7.54	0.871	3053	0.54
Al	0.37	1.82	1064	30	0.81	11.4	6.19	0.681	3034	0.31
Al	0.48	0.838	1064	35	0.73	6.13	6.76	0.336	2841	0.13
Al	0.52	0.502	1064	37	0.71	15.3	7.61	0.745	2993	0.29
Al	0.57	1.89	1064	39	0.68	5.78	6.75	0.317	2833	0.10
Al	0.71	0.848	1064	46	0.65	5.97	5.77	0.383	2892	0.084
Al	0.75	2.70	1064	47	0.63	3.10	6.52	0.176	2775	0.041
Al	5.02	2.858	527	268	0.53	15.6	6.57	0.880	3118	0.031
Al	6.38	1.855	527	315	0.49	10.6	7.89	0.497	2882	0.017
Al	6.63	1.857	527	323	0.49	9.96	6.73	0.548	2939	0.015
where $\rho_o = 2700$ kg/m^3										
Fe	0.58	0.884	1064	41	0.71	0.353	1.15	0.0390	8146	0.0061
Fe	5.11	0.914	527	278	0.54	31.7	5.90	0.682	8899	0.062
where $\rho_o = 7870$ kg/m^3										
Ni	0.29	1.002	1064	26	0.90	0.178	0.640	0.0313	9358	0.0061
Ni	12.3	1.002	527	496	0.40	115	5.45	2.38	15800	0.093
Ni	13.4	1.002	527	525	0.39	163	5.48	3.34	22790	0.12
where $\rho_o = 8900$ kg/m^3										
Dunite	0.32	1.01	1064	27	0.84	16.4	8.21	0.781	2818	0.51
Dunite	0.65	1.00	1064	44	0.68	29.2	8.00	1.43	3105	0.45
Dunite	4.37	2.32	527	250	0.57	18.8	9.96	0.742	2755	0.043
Dunite	5.51	1.00	527	290	0.53	15.3	8.55	0.704	2779	0.028
where $\rho_o = 2550$ kg/m^3										
CV3	0.58	1.61	1064	40	0.69	0.248	1.72	0.0495	2296	0.0043
CV3	4.89	1.73	527	270	0.55	0.734	1.52	0.166	3267	0.0015
CV3	5.18	1.71	527	280	0.54	0.600	2.80	0.0736	2989	0.0012

where $\rho_o = 2910$ kg/m^3

Graphite	0.20	0.975	1064	20	1.00	4.27	3.33	0.712	2290	0.21
Graphite	0.38	0.986	1064	30	0.79	1.62	2.92	0.309	2013	0.043
Graphite	0.42	0.996	1064	33	0.78	2.93	2.62	0.621	2359	0.0070
Graphite	0.42	0.978	1064	33	0.78	3.23	2.47	0.726	2549	0.0077
Graphite	0.46	0.970	1064	35	0.76	2.05	2.28	0.499	2304	0.0045
Graphite	3.76	0.998	527	220	0.58	0.922	2.80	0.183	1926	0.0024

where $\rho_o = 1800$ kg/m^3

Table 1. Aluminum, iron, nickel, dunite, CV3 (meteorite), and graphite targets are listed in terms of the input intensity, I (TW/cm^2), target thickness, δ(mm), laser irradiation wavelength, λ(nm), plasma pressure inducing momentum transfer, P_{pl} (GPa), plasma momentum coupling coefficient, $C_{M\,pl}$ (s/m x 10^{-5}), Hugoniot rear surface pressure, P_H (GPa), shock wave velocity, u_s (km/s), particle velocity, u_p (km/s), compressed density, ρ (kg/m^3), and rear surface momentum coupling coefficient $C_{M\,H}$ (s/m x 10^{-5}).

P_H (GPa)	u_s (km/s)	u_p (km/s)	ρ (kg/m^3)	c (km/s)
0.0	*5.33*	*0.0*	*2785*	*5.328*
3.10	**6.52**	**0.176**	**2775**	
4.5	*5.78*	*0.279*	*2925*	
5.78	**6.75**	**0.317**	**2833**	
5.97	**5.77**	**0.383**	**2892**	
6.13	**6.76**	**0.336**	**2841**	
9.96	**6.73**	**0.548**	**2939**	
10.0	*6.11*	*0.587*	*3081*	*6.220*
10.6	**7.89**	**0.497**	**2882**	
11.4	**6.19**	**0.681**	**3034**	
15.0	*6.42*	*0.839*	*3204*	
15.3	**7.61**	**0.745**	**2993**	
15.6	**6.57**	**0.880**	**3118**	
17.7	**7.54**	**0.871**	**3053**	
20.0	*6.75*	*1.06*	*3306*	*6.849*

Table 2. Comparison for NLS aluminum (pure) Hugoniot pressures between laser generated and optical deflection measured EOS variables (bold print) with those obtained from gas gun (italics) for aluminum 2024 alloy. The trend agreement is fair, with scatterings as anticipated, over the range measured; c is the speed of sound in the material.

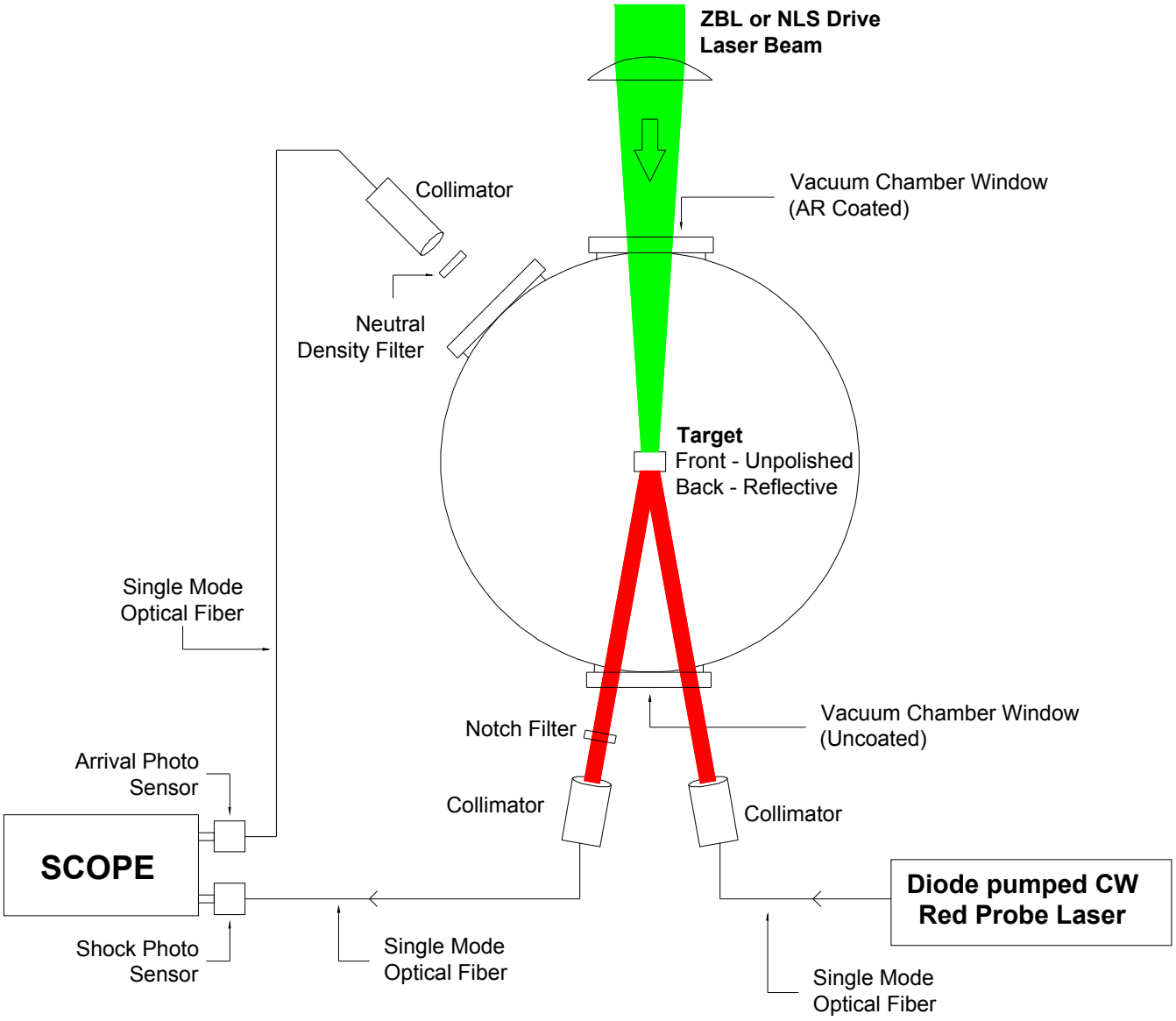

Typical Al Target Reflectivity Response for NLS Laser (1064 nm) Irradiation

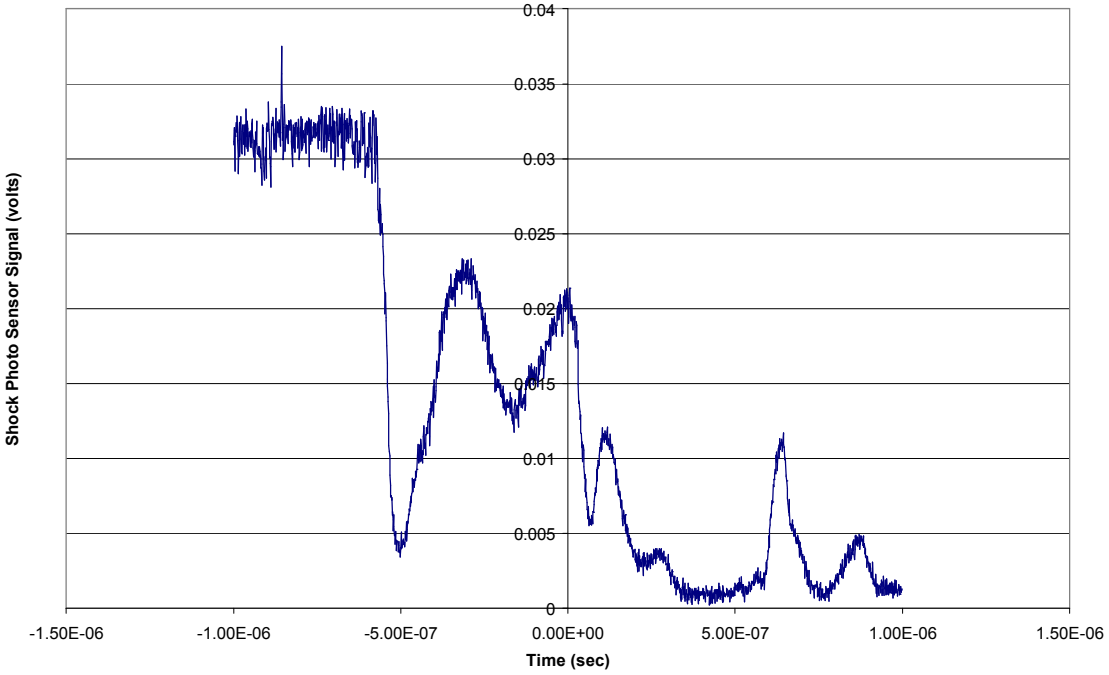

Typical Al Target Reflectivity Response for ZBL Laser (527 nm) Irradiation

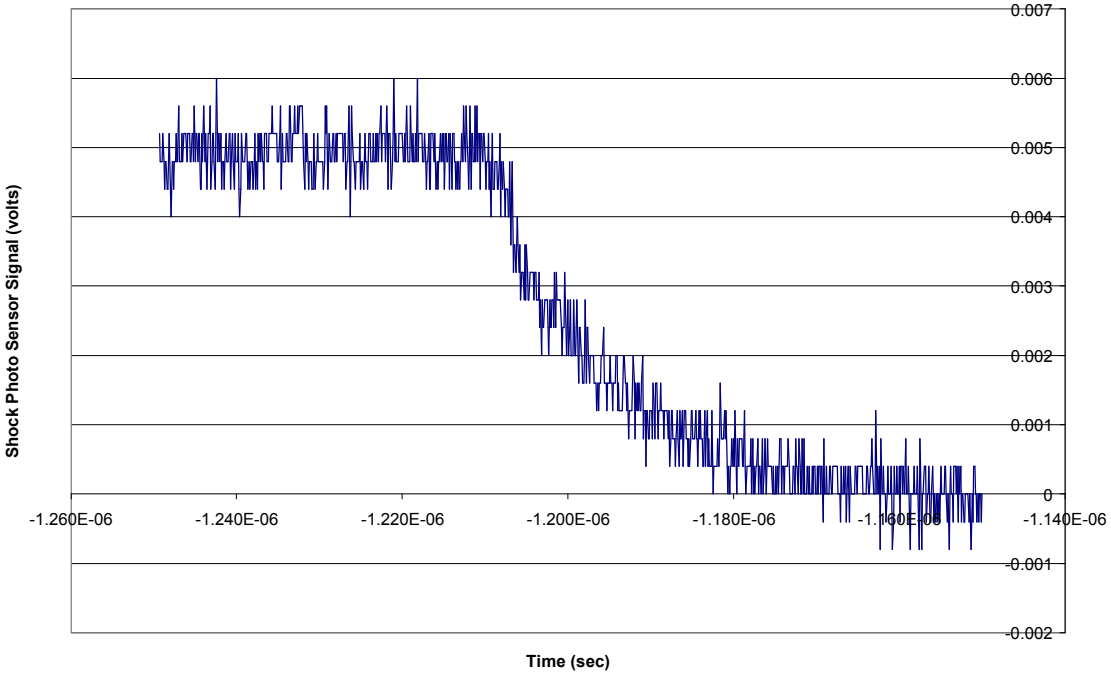

Aluminum Shock Wave Speed as a Function of Hugoniot Pressure

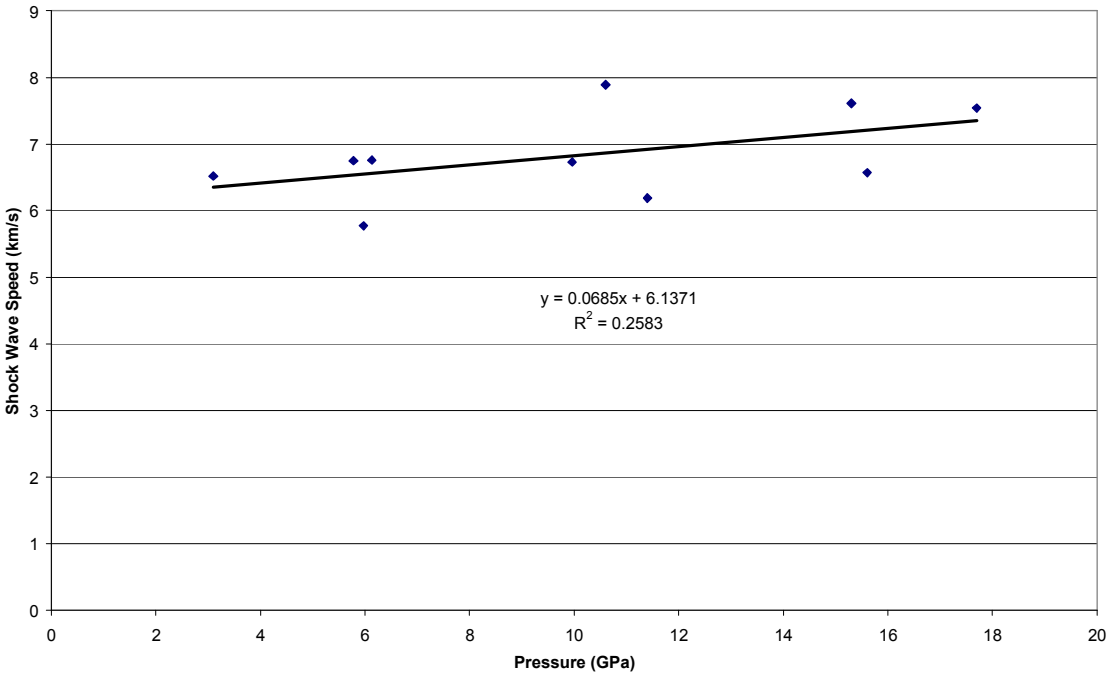

Aluminum Particle Speed as a Function of Hugoniot Pressure

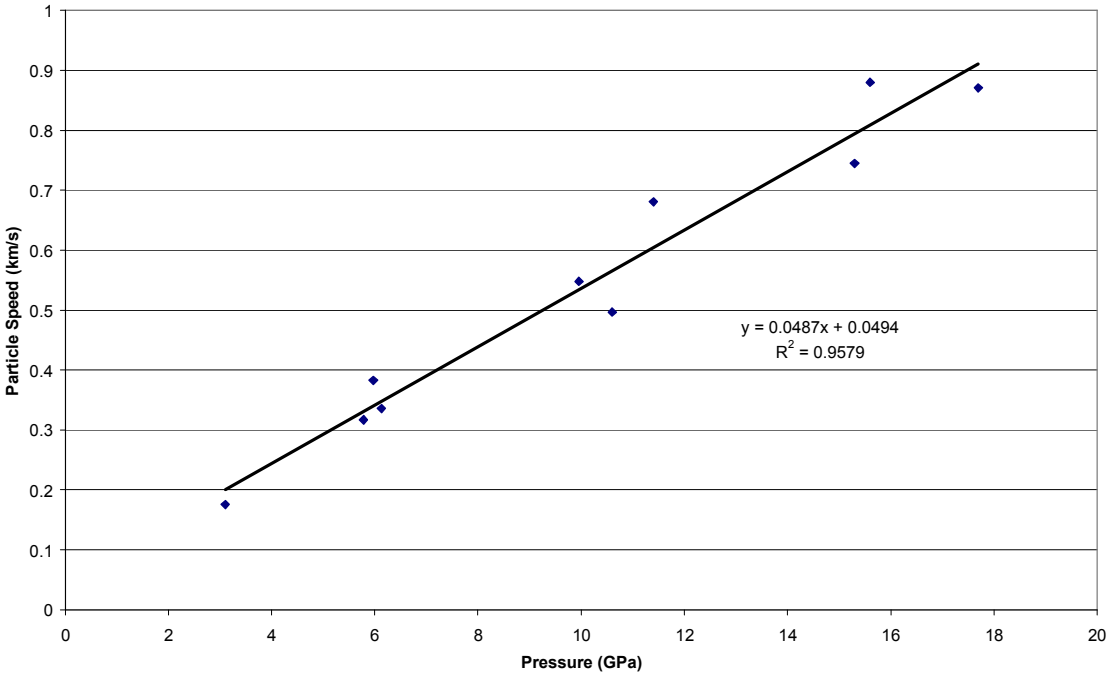

Aluminum Compressed Density as a Function of Hugoniot Pressure

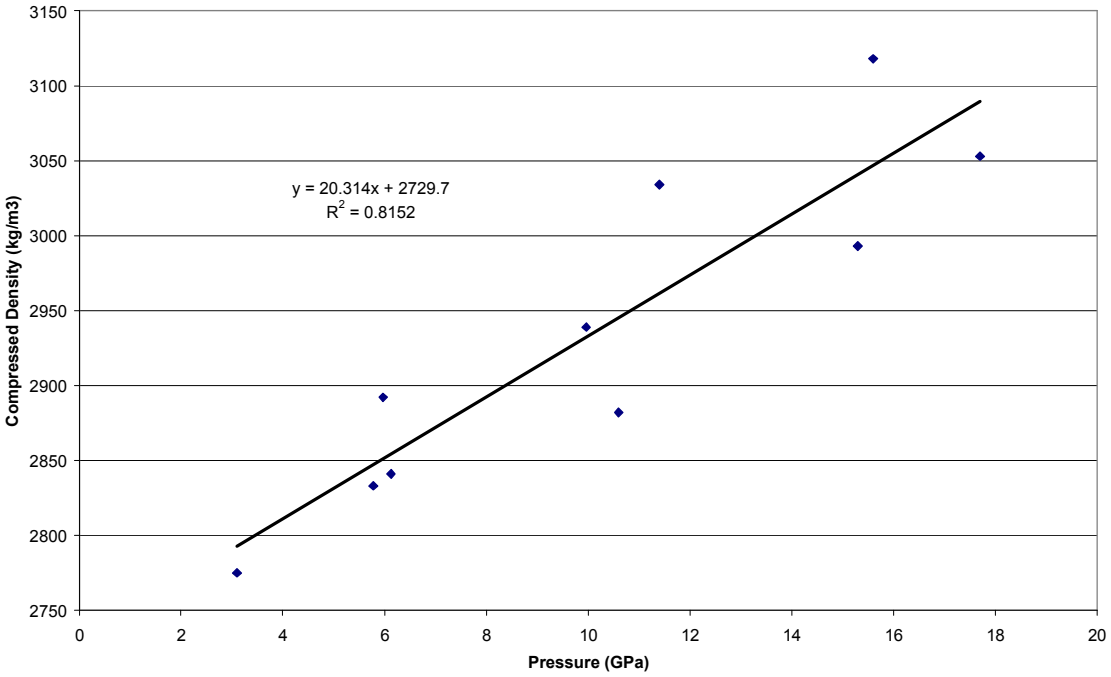

Aluminum Momentum Coupling Coefficient as a Function of Laser Irradiation Intensity